Effects of DJ-1 on apoptosis and mitophagy of glomerular podocytes

JING XIAO[1,2*], JUNJIE TAN[1,3*], LI YU[1,3], GUOSHENG LIU[1] and SHENGYOU YU[1,3]

[1]Department of Pediatrics, The First Affiliated Hospital of Jinan University, Guangzhou, Guangdong 510630; [2]Department of Pediatrics, Affiliated Hospital of Guangdong Medical University, Zhanjiang, Guangdong 524002; [3]Department of Pediatrics, Guangzhou First People's Hospital, The Second Affiliated Hospital of South China University of Technology, Guangzhou, Guangdong 510180, P.R. China

Received March 10, 2023; Accepted July 14, 2023

DOI: 10.3892/etm.2023.12162

Abstract. By studying the effects of DJ-1 overexpression and silencing on the morphological structure and mitophagy of glomerular podocytes, the present study aimed to identify the effects of DJ-1 on glomerular podocyte apoptosis and mitophagy. MPC5 mouse glomerular podocytes were cultured *in vitro* and divided into four groups: Control, DJ-1 overexpression, empty vector and DJ-1 silencing. DJ-1 gene overexpression and silencing models were prepared, the morphological structures of podocytes and mitochondria in each group were observed, and podocyte apoptosis and DJ-1/PTEN expression were subsequently detected in each group. The experimental results showed reduced volume, retracted foot processes, loosened intercellular connections, presence of dead cells, increased apoptotic rate, increased expression of PTEN, and swollen mitochondria due to the number of vacuoles and autophagosomes in podocytes in the DJ-1 silencing group. The surface areas of podocytes in the DJ-1 overexpression group were greater than those in the control group. Moreover, the structure of the foot processes was more obvious, the number of cells was greater, the intercellular connections were closer, the apoptotic rate was reduced, the expression of PTEN was decreased, the mitochondrial structure was more obvious and the mitochondrial cristae were more whole. Notably, there were no differences between the empty vector and control groups. In conclusion, these results indicated that DJ-1 may regulate podocyte apoptosis and mitophagy through the DJ-1/PTEN pathway, and could maintain the stability of the normal morphology, structure and function of glomerular podocytes.

Correspondence to: Professor Li Yu or Professor Guosheng Liu, Department of Pediatrics, The First Affiliated Hospital of Jinan University, 613 Huangpu Avenue West, Tianhe, Guangzhou, Guangdong 510630, P.R. China
E-mail: jnuped@126.com
E-mail: jnuped@163.com

*Contributed equally

Key words: DJ-1, PTEN, podocytes, mitochondria, autophagy, proteinuria

Introduction

Podocytes, the visceral epithelial cells of the renal capsule, attach to the outside of the glomerular basement membrane, and together with vascular endothelial cells and the glomerular basement membrane, constitute the glomerular hemofiltration barrier. The foot processes between podocytes are bridged by the slit diaphragm. The morphological and structural integrity of podocytes is crucial for maintaining the normal function of glomerular basement membrane cells (1). Glomerular podocyte dysfunction, due to factors such as oxidative stress, genetic mutations and inflammation, can lead to protein leakage into the urine, resulting in proteinuria. Podocyte injury is a common cause of glomerular disease and a hallmark of disease progression (2).

DJ-1 is a member of the peptidase C56 protein family encoded by the PARK7 gene, which is mainly present in the heart, liver, kidney, skeletal muscle, gonads and other organs. It is a critical functional protein in the apoptotic signal transduction pathway and is involved in cell metabolism and energy conversion (3). Mitophagy is a physiological process that selectively eliminates damaged mitochondria to promote mitochondrial renewal and maintain a regular supply of intracellular energy (4). PTEN is an upstream regulatory protein of signaling pathways, such as PTEN-induced putative kinase 1 (PINK1)/Parkin and PI3K/Akt/mTOR, which specifically regulate mitophagy and participate in mitochondrial homeostasis (5). Mitochondria are significant producers of reactive oxygen species (ROS) in cells. Several studies have suggested that DJ-1 is an upstream regulator of PTEN and that DJ-1 acts as a sensitive oxidative stress sensor *in vivo* (6,7). When DJ-1 reacts with intracellular ROS, its molecular conformation significantly changes. This change can increase DJ-1 protein levels; the binding of DJ-1 and ROS regulates PTEN function, and affects mitophagy and cellular energy supply (8). The kidney possesses one of the highest rates of energy metabolism out of all the organs in the body and mitochondria are essential

for the protection of kidney function. With the progression of molecular experimental methods, such as PCR and western blotting, mitophagy has gradually become a new focus of research in elucidating the pathogenesis of kidney disease (9).

Few previous studies have investigated how DJ-1 regulates the physiological function of glomerular podocytes (10,11). It has been suggested that autophagy activation and the inhibition of apoptosis have protective effects in high glucose-induced podocyte injury models, and that this protective effect is associated with DJ-1 (12). Our preliminary study indicated that podocyte injury and DJ-1 expression are positively associated (10). However, the specific mechanism underlying the regulatory effects of DJ-1 on podocyte function remains to be elucidated; therefore, the present study aimed to clarify this. In the present study, mouse glomerular podocyte DJ-1 gene overexpression and silencing models were constructed to further explore the role and significance of DJ-1 in maintaining podocyte morphological structure and mitophagy.

Materials and methods

Podocyte culture. MPC5 mouse glomerular podocytes were purchased from BeNa Culture Collection; Beijing Beina Chunglian Institute of Biotechnology and were stored in liquid nitrogen. Before the experiment, podocytes were recovered, collected, and cultured in RPMI 1640 medium (Gibco; Thermo Fisher Scientific, Inc.) containing antibiotics (1% penicillin and streptomycin) and 10% FBS (Gibco; Thermo Fisher Scientific, Inc. at 33˚C in a humidified 5% CO_2/95% air atmosphere. Recombinant mouse γ-interferon (10 U/ml, BINDER GmbH) was used to induce podocyte proliferation. After podocyte confluence reached 80-90%, 0.25% trypsin/0.02% EDTA (Gibco; Thermo Fisher Scientific, Inc.) was added. Subsequently, the podocytes were moved to a 37˚C environment for differentiation and maturation for 10-14 days. The differentiated and matured podocytes were then seeded into six-well plates (Corning), and after the cells reached 60-70% confluence, RPMI 1640 alone was used to starve the podocytes for 12 h to synchronize the proliferation of the cells, before the experimental grouping was performed.

Experimental grouping. Podocytes were randomly divided into the following four groups: i) Control group, cells were cultured in RPMI 1640; ii) DJ-1 overexpression (OE) group (OE-DJ-1), cells were transfected with the OE-DJ-1 plasmid; iii) empty vector group, cells were transfected with an empty vector as a negative control; iv) DJ-1 silencing group (Si-DJ-1), cells were transfected with small interfering RNA (siRNA)-DJ-1 for gene silencing.

Model establishment

Overexpression. Cells were passaged 1 day before transfection, and transfection was conducted using Lipofectamine® 2000 transfection reagent (cat. no. 11668019l; Invitrogen; Thermo Fisher Scientific, Inc.) according to the manufacturer's instructions. When cell confluence reached 70-80%, 3 μg OE-DJ-1 plasmid [pcDNA3.1(+), Invitrogen; Thermo Fisher Scientific, Inc.] or empty vector and AB mixture were added to each well of a 6-well plate where cells were seeded; solution A refers to 100 μl Opti-MEM cell culture medium (cat. no. 31985070; Gibco; Thermo Fisher Scientific, Inc.) and solution B refers to 3 μl Lipofectamine 2000 solution dissolved in Opti-MEM medium. The cells were transfected at 37˚C in a 5% CO_2 atmosphere for 5 h. Subsequently, the cells were cultured in complete medium at 37˚C and DJ-1 expression was detected after 48 h.

Silencing. Podocytes in the logarithmic growth phase were selected, the cell suspension was adjusted to a density of $1x10^5$/ml following trypsinization and the cells were inoculated into six-well plates. Subsequently, 20 μm siRNA storage solution was added to Opti-MEM medium to reach final concentrations of 100, 50 and 25 nM, which was designated as solution A. Then, 10 μl Lipofectamine 2000 transfection reagent was added to 100 μl Opti-MEM medium as solution B. Solutions A and B were mixed and incubated at room temperature for 15-20 min to prepare the transfection complex. The transfection complex was then added to complete medium, which was added to a 6-well plate with a final volume of 2 ml (100 nM) per well. After 5 h of incubation of cells at 37˚C, the medium was replaced with cell culture medium. After 24 h of transfection, the culture medium was discarded, and washed twice with PBS.

Detection of transfection efficiency. To verify the transfection efficiency of OE-DJ-1 and Si-DJ-1, reverse transcription-quantitative PCR (RT-qPCR) was used to detect the mRNA expression levels of DJ-1 in cells compared with those in cells transfected with the empty vector or si-NC (cat. no. siN0000001-1-5; Guangzhou RiboBio Co., Ltd.).

Podocyte morphology. Podocyte morphology was observed using an inverted phase-contrast microscope (Axio Vert 25; Carl Zeiss AG) at a magnification of x200.

Flow cytometry-based apoptosis assay. After rinsing MPC-5 cells with pre-cooled PBS, EDTA-free trypsin was added to digest the cells and the suspended cells were collected. The cells were centrifuged at room temperature for 5 min (400 x g), the supernatant was removed, rinsed twice with pre-cooled PBS and the cells were collected. Cells ($1x10^6$) were added to 400 μl binding buffer (BioVision, Inc.) to resuspend the cells, after which, 10 μl annexin V-FITC (BioVision, Inc.) and 5 μl PI (BioVision, Inc.) were added, and allowed to stand at room temperature for 10 min in the dark. Subsequently, flow cytometry (FACSCanto; BD Biosciences) was conducted and data were analyzed using FlowJo-V10 software (FlowJo LLC).

RT-qPCR. Total RNA was extracted according to the instructions of the RNAgents® Total RNA Isolation System (Promega Corporation) (13). Then, the purity and integrity of the total RNA was detected. Briefly, the purity of the RNA was detected by measuring the OD 260/OD 280 ratio with a nucleic acid protein analyzer (BioPhotometer Plus; Shanghai Musen Biotechnology Co., Ltd.). The integrity of the total RNA was assessed by 1% agarose gel electrophoresis, which was performed at 80 V for 20 min, and the total RNA bands were observed with a gel imaging system (Zhuhai Hema Medical Instrument Co., Ltd.). Thereafter, the extracted

RNA was transcribed into cDNA using PrimeScript™ RT Master Mix Kit (Takara Bio, Inc.) according to the manufacturer's protocol. SYBR Premix Ex Taq™ II (Takara Bio, Inc.) was used for qPCR and reactions were performed using a LightCycler480 Real-Time PCR System (Roche Diagnostics) with the following protocol: 95˚C for 5 min, followed by 40 cycles at 95˚C for 15 sec, 60˚C for 15 sec and 72˚C for 30 sec. The primer sequences were as follows: DJ-1 forward, 5' AACACACCCACTGGCTAAGG 3', reverse, 5' GGCTAG TGCAAACTCAAAGC 3'; PTEN forward, 5'-TGAGTTCCC TCAGCCATTGCCT-3', reverse, 5'-GAGGTTTCCTCTGGT CCTGGTA-3'; and β-actin forward, 5' ACATCCGTAAAG ACCTCTATGCC 3', reverse, 5' TACTCCTGCTTGCTGATC CAC 3'. Primers were designed and synthesized by Shanghai Sangon Bioengineering Co., Ltd. Data were calculated using the $2^{-\Delta\Delta Cq}$ method (14).

Western blot analysis. The MPC-5 cells in each group were rinsed twice with PBS, and the PBS was aspirated prior to the addition of RIPA cell lysis solution (Thermo Fisher Scientific, Inc.). The cells were then shaken on ice for 30 min and lysed by pipetting. Total protein concentration was measured using the BCA method and the proteins were denatured at 100˚C for 10 min. Total proteins (30 μg) were separated by SDS-PAGE on 12% gels and were transferred to PVDF membranes. Blocking was performed with 5% nonfat milk powder at 25˚C on a shaker for 2 h, after which, dropwise rabbit anti-DJ-1 (1:1,000; cat. no. ab76008; Abcam), rabbit anti-PTEN (1:1,000; cat. no. ab137337; Abcam), rabbit anti-LC3B (1:1,000; cat. no. ab192890; Abcam), rabbit anti-Bad (1:1,000; cat. no. ab32445; Abcam) or rabbit anti-GAPDH (1:1,000; cat. no. ab9485; Abcam) antibodies were added, and incubated overnight at 4˚C on a shaker. The horseradish peroxidase-conjugated secondary antibody (1:1,000; cat. no. ab6721; Abcam) was then added for 1 h at room temperature on a shaker. Subsequently, 1 ml western blot ECL reagent (MilliporeSigma) was added to the blots, which were exposed, and images were captured. The exposed image was scanned using ImageJ (V1.8.0; National Institutes of Health) and the gray value of the protein band was analyzed.

Immunofluorescence staining and confocal laser scanning microscopy. MPC-5 cells were cultured and separated into groups. Subsequently, the cells were fixed with 4% paraformaldehyde at 4˚C for 8 min, ruptured with Triton-100 at room temperature for 5 min and blocked with 5% BSA (Gibco; Thermo Fisher Scientific, Inc.) at 37˚C for 1 h. Subsequently, DJ-1 (1:50; cat. no. ab76008; Abcam) or PTEN (1:50; cat. no. ab137337; Abcam) primary antibodies were added dropwise to the cell slides, and the cells were incubated in a humidified atmosphere at 4˚C overnight. After washing three times with PBS, an Alexa Fluor™ 568 goat anti-rabbit secondary antibody (1:200; cat. no. A11011; Invitrogen; Thermo Fisher Scientific, Inc.) was added and incubated at 37˚C for 1 h, and nuclear staining was performed with 0.1% DAPI at room temperature for 10 min. Excess DAPI was washed three times with PBS-0.1% Tween, the slides were sealed with a mounting solution containing anti-fluorescence quencher, and the cells were observed under a fluorescence microscope. To semi-quantify DJ-1 and PTEN levels in the cells, three typical images from each group were analyzed by ImageJ based on a reported method (15).

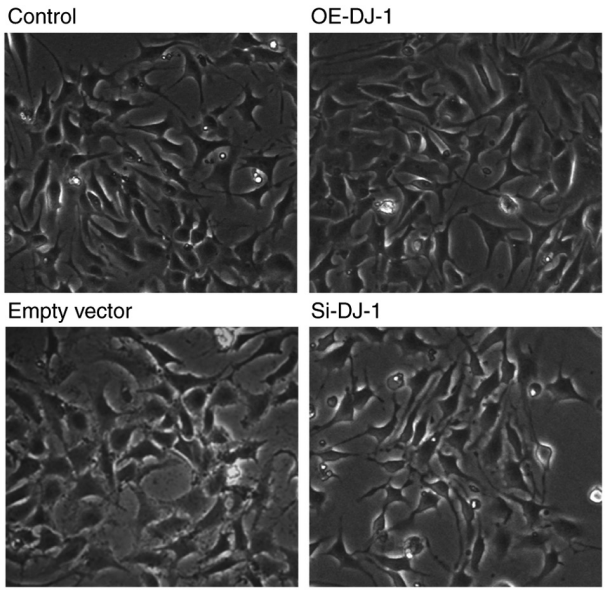

Figure 1. Morphological analysis of glomerular podocytes (magnification, x200). OE, overexpression; Si, silencing.

Transmission electron microscopy. Podocytes from each group were collected, fixed with glutaraldehyde and 1% osmium tetroxide for 15-30 min at 4˚C, and dehydrated at room temperature with gradient concentrations of acetone. The dehydrated samples were embedded in pure acetone-EPON812 embedding medium for 2 h at room temperature, baked to solidify, sectioned (1 μm), stained dropwise with sodium acetate for 30 min at room temperature and washed with PBS. Samples were imaged using a transmission electron microscope (Libra 120 microscope; Carl Zeiss AG) to observe autophagosomes.

Statistical analyses. All experiments were repeated at least three times. All data were statistically processed using SPSS17.0 statistical software (SPSS, Inc.). The measurement data are expressed as the mean ± standard deviation. Unpaired Student's t-test was used for comparisons between two groups, and one-way ANOVA followed by Tukey's post hoc test was used for comparisons among multiple groups. $P<0.05$ was considered to indicate a statistically significant difference.

Results

Morphological changes of podocytes. As shown in Fig. 1, there were differences in cell morphology among the different treatment groups. There was no marked difference in cell morphology between the empty vector and control groups. Compared with the control group, the podocytes in the OE-DJ-1 group exhibited a larger volume, more obvious foot processes, more regularly shaped nuclei, and tight junctions between adjacent cells, whereas the podocytes in the Si-DJ-1 group exhibited a decrease in volume and the foot processes contracted inward. Neighboring cells were loosened and some

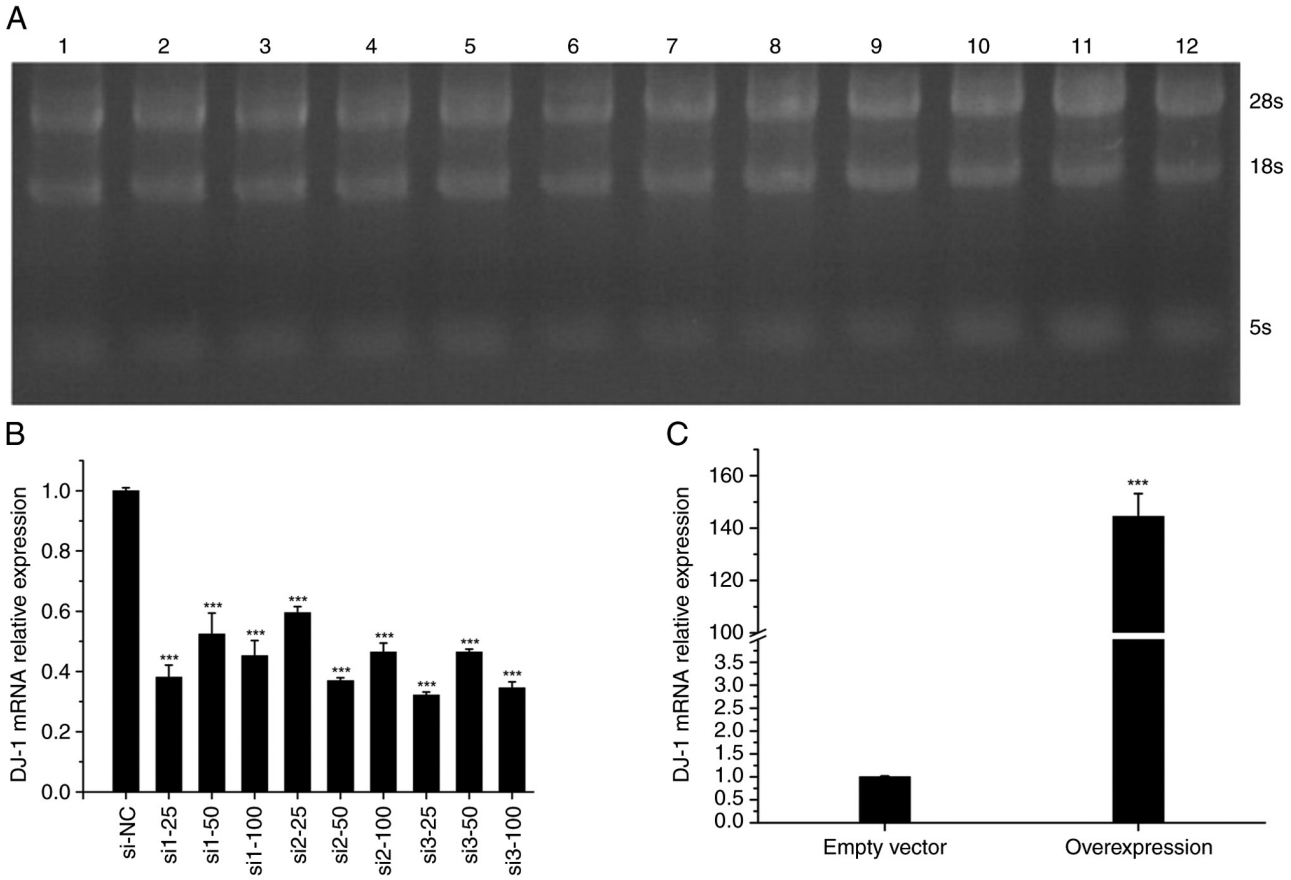

Figure 2. (A) RNA electrophoresis of 12 samples. Lane 1, si1-25; lane 2, si1-50; lane 3, si1-100; lane 4, si2-25; lane 5, si2-50; lane 6, si2-100; lane 7, si3-25; lane 8, si3-50; lane 9, si3-100; lane 10, si-NC; lane 11, OE-DJ-1; lane 12, empty vector. (B) DJ-1 mRNA expression in 10 silencing samples. ***P<0.05 vs. si-NC. (C) DJ-1 mRNA expression in the overexpression group and the empty vector group. ***P<0.05 vs. empty vector. OE, overexpression; NC, negative control; si, small interfering.

dead cells were observed. The morphology of podocytes observed in the present study is in line with findings from previous studies (16,17).

Podocyte transfection efficiency. After assessing three different siRNA transfection concentrations, the optimal concentration required was determined. Agarose gel electrophoresis (Fig. 2A) showed that the RNA extracted had high purity and contained no DNA contamination or degradation. Podocytes were treated with different DJ-1 siRNA transfection concentrations (25, 50 and 100 nM). Compared with in the si-NC group, the expression levels of DJ-1 were significantly reduced after transfection with Si-DJ-1 (P<0.05; Fig. 2B), and there were no obvious differences among the different transfection concentrations and siRNAs used. Therefore, 25 nM si3 was selected as the experimental working concentration for subsequent silencing. Furthermore, the expression levels of DJ-1 in the OE-DJ-1 group were significantly increased compared with those in the empty vector group (Fig. 2C).

Changes in podocyte apoptosis rate. The apoptotic rate of podocytes (Fig. 3A; quadrants 2 and 3) in the control group and empty vector group was lower than that in the Si-DJ-1 group ((P<0.05; Fig. 3A), and there was no significant difference between the control and empty vector groups; however, the apoptotic rate of the control group and the empty group was significantly higher than that in the OE-DJ-1 group (P<0.05; Fig 3A). In addition, compared with those in the control group and empty vector group, the expression levels of the proapoptotic protein Bad were significantly reduced in the OE-DJ-1 group, whereas they were significantly increased in the Si-DJ-1 group (P<0.05; Fig. 3B).

mRNA expression levels of DJ-1 and PTEN in podocytes. The results of qPCR showed that the relative mRNA expression levels of DJ-1 in the control and empty vector groups were lower than those in the OE-DJ-1 group. Moreover, DJ-1 expression was significantly higher in the OE-DJ-1 group than that in the control group (P<0.05), whereas it was significantly lower in the Si-DJ-1 group than that in the control group (P<0.05) (Fig. 4A). The relative mRNA expression levels of PTEN were significantly lower in the OE-DJ-1 group than those in the control group (P<0.05) and were significantly higher in the Si-DJ-1 group (P<0.05; Fig. 4B).

Protein expression levels of DJ-1 and PTEN in podocytes. Western blotting results showed no significant difference in the protein expression levels of DJ-1 between the control and empty vector groups. The protein expression levels of DJ-1 were significantly higher in the OE-DJ-1 group than those in

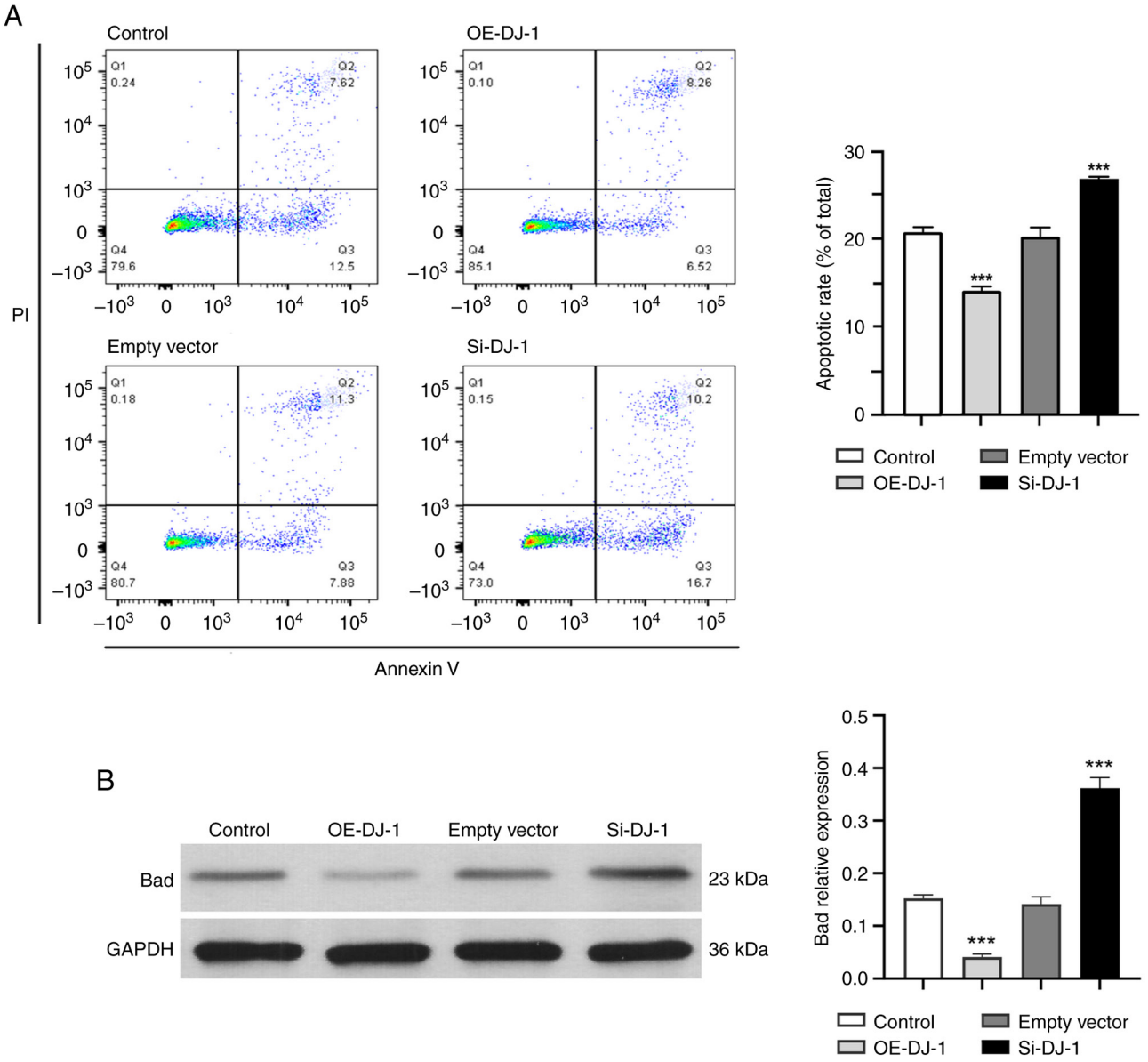

Figure 3. (A) Apoptotic rate of podocytes was detected by flow cytometry. Q1, PI (+) and annexin V (-), necrotic/dead cells; Q2, PI (+) and annexin V (+), late apoptotic or dead cells; Q3, PI (-) and annexin V (+), early apoptotic cells; Q4, annexin V (-) and PI (-), normal living cells. (B) Expression of the proapoptotic protein Bad in each group. ***P<0.05 vs. control group. OE, overexpression; Si, silencing.

the control group (P<0.05). By contrast, the protein expression levels of DJ-1 were significantly lower in the Si-DJ-1 group than those in the control group (P<0.05; Fig. 5A). The protein expression levels of PTEN were relatively low in both the control and empty vector groups. The protein expression levels of PTEN were significantly lower in the OE-DJ-1 group than those in the control group (P<0.05). By contrast, the protein expression levels of PTEN were significantly increased after DJ-1 gene silencing compared with those in the control group (P<0.05; Fig. 5B).

Distribution of DJ-1 and PTEN proteins. The DJ-1 protein was evenly distributed throughout the cell membrane in the control and empty vector groups, and there was no significant difference between the two groups. In the OE-DJ-1 group, the expression of DJ-1 was significantly higher than that in the control group (P<0.05; Fig. 6A). In the Si-DJ-1 group, the expression of DJ-1 was significantly reduced, compared with that in the control group (P<0.05; Fig. 6A).

In the control and empty vector groups, PTEN was mainly distributed discontinuously on the surface of the cell membrane, a small amount of PTEN was evenly distributed in the cytoplasm, and granular distribution was also observed around the nucleus. When DJ-1 was overexpressed, the distribution of PTEN in the cell membrane was markedly reduced, and a granular uneven distribution was observed in the cytoplasm. The difference in PTEN expressions levels was statistically significant compared with that in the control group (P<0.05; Fig. 6B). In addition, the distribution of PTEN in the cell membrane and cytoplasm of the cells in the Si-DJ-1 group was notably increased, and evenly and densely distributed in clumps, with a statistically significant difference in PTEN expression levels compared with those in the control group (P<0.05; Fig. 6B).

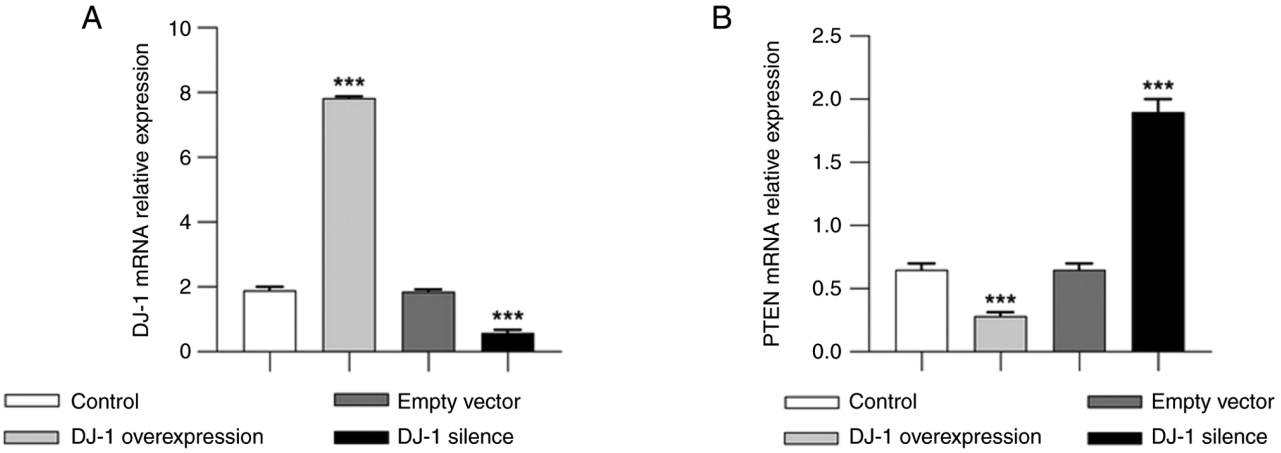

Figure 4. mRNA expression levels of (A) DJ-1 and (B) PTEN in podocytes in each group. ***P<0.05 vs. control group.

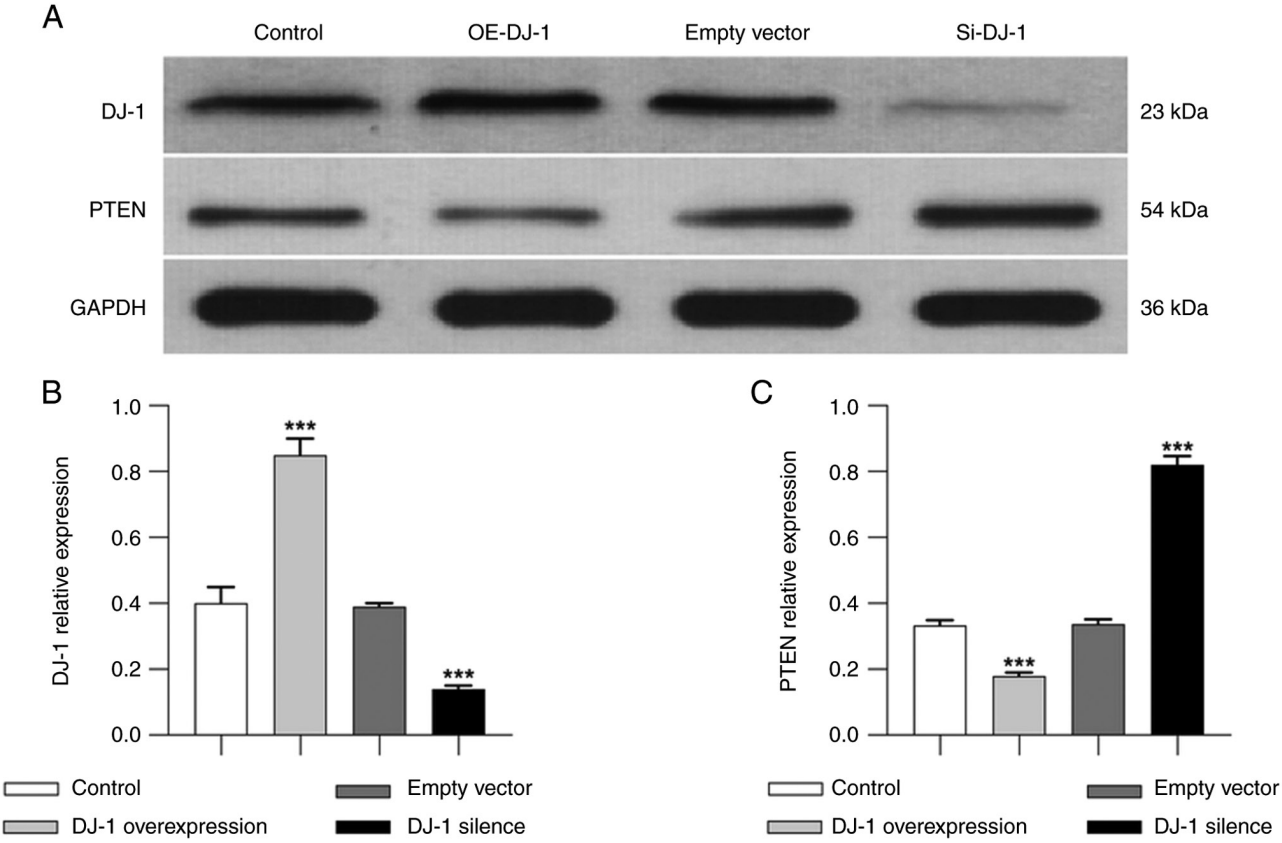

Figure 5. (A) Western blot analysis of DJ-1 and PTEN protein expression in podocytes. Semi-quantification of (B) DJ-1 and (C) PTEN protein expression compared with the control group. ***P<0.05 vs. control group. OE, overexpression; Si, silencing.

Mitochondrial morphology and autophagosomes. In the control and empty vector groups, the structure of most mitochondria was clear and the mitochondrial cristae were complete. The structure of the mitochondria in the OE-DJ-1 group was relatively clear and the mitochondrial cristae were complete, similar to the control group. In the Si-DJ-1 group, the mitochondrial structure was swollen, mitochondrial cristae were scattered, vacuoles appeared and the number of autophagosomes was markedly increased (Fig. 7A). Compared with the control group, the expression levels of the autophagy marker LC3B were significantly increased in the Si-DJ-1 group (P<0.05; Fig. 7B).

Discussion

The DJ-1 gene, also known as PARK7, is located on chromosome 1p36.23. It is widely expressed in various tissues in eukaryotic and prokaryotic organisms, it encodes the DJ-1 protein and belongs to the C56 peptidase family. DJ-1 is a nucleic acid disaccharidase with a molecular weight of ~20 kDa and contains 189 amino acids, existing as a homodimer (18). Oxidative stress promotes the dissociation of cytoplasmic DJ-1 dimers into monomers that are translocated to the nucleus. DJ-1 acts as a co-activator of various signaling pathways and

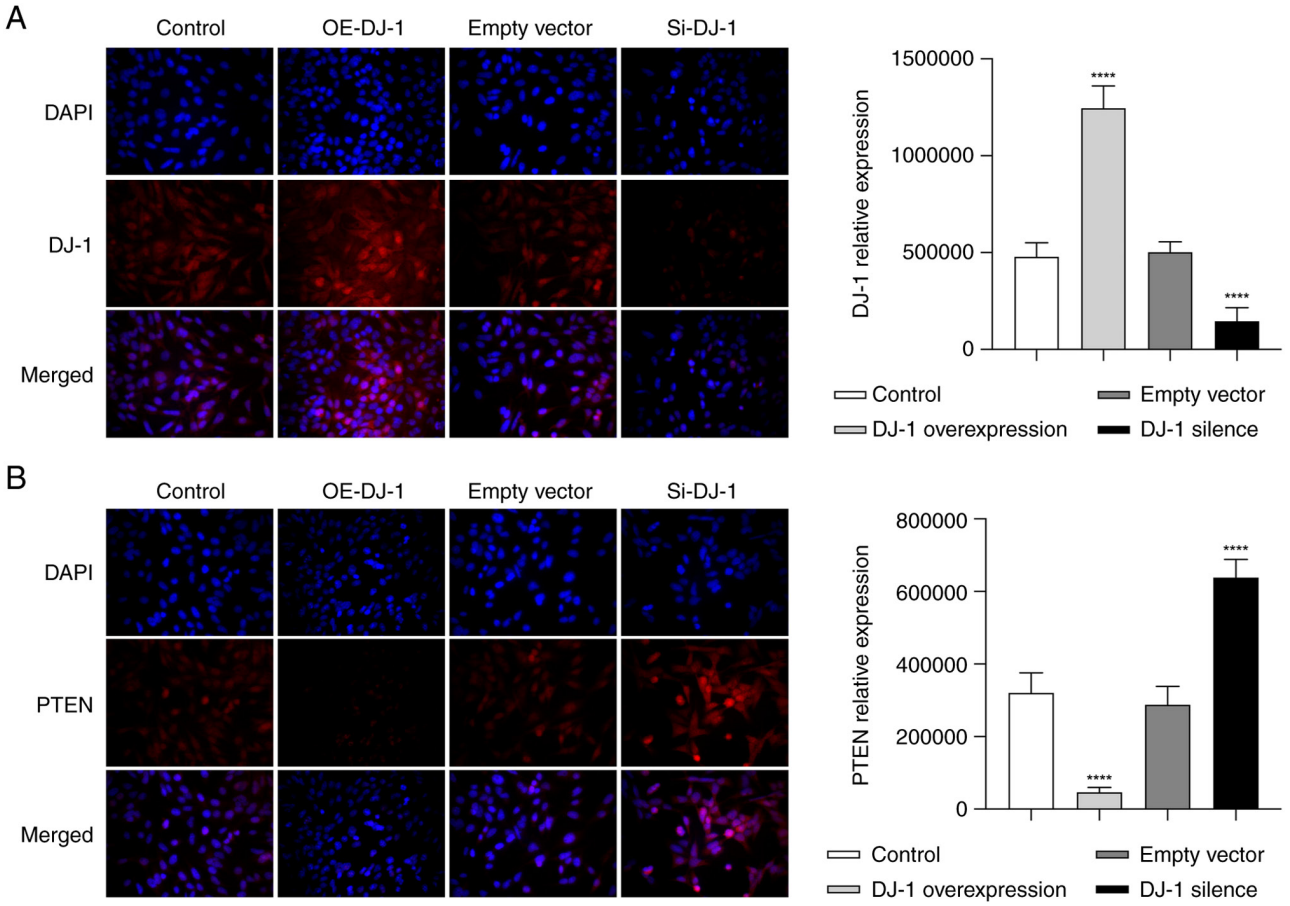

Figure 6. Immunofluorescence analysis of (A) DJ-1 and (B) PTEN protein distribution (magnification, x400). ****P<0.01 vs. control group. OE, overexpression; Si, silencing.

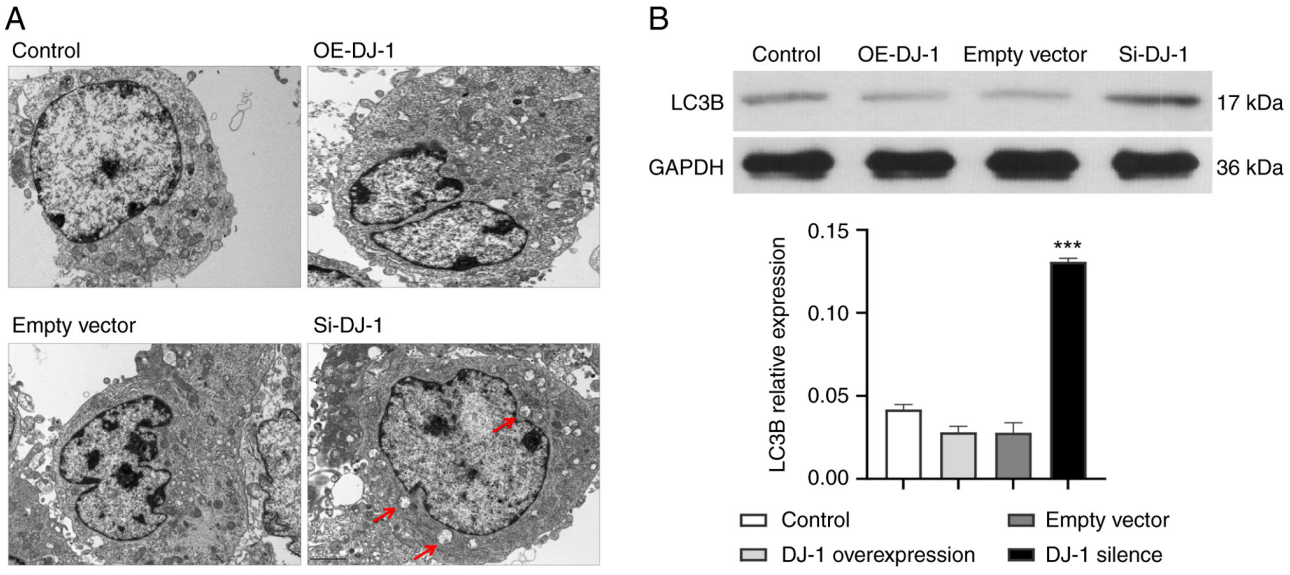

Figure 7. (A) Distribution of podocyte autophagosomes detected by electron microscopy (red arrow; magnification, x13,500). (B) Expression levels of the autophagy marker protein LC3B in podocytes in each group. ***P<0.05 vs. control group. OE, overexpression; Si, silencing.

regulates cell death in the nucleus (19). The crystal structure of human DJ-1 contains three cysteine residues at amino acids 46, 53 and 106 (Cys46, Cys53 and Cys106), which is its main functional domain. Notably, DJ-1 is a sensitive oxidative stress sensor *in vivo* and can determine the intracellular redox level according to its different oxidation states [non-oxidation, $SO2^-$ (free radical), $SO3^-$ (free radical)] (20). DJ-1 has powerful anti-oxidative, immunoregulatory, anti-apoptotic and

molecular chaperone functions (21). Its adaptive regulation of cells under oxidative stress is attributed to its regulation of multiple signal transduction pathways, especially its neuroprotective effect (22). Previous studies have shown that DJ-1 can improve cell survival and induce proliferation by activating ERK1/2 and PI3K/Akt signaling pathways, and nuclear factor erythroid 2-related factor 2 pathway-mediated antioxidant responses, and can attenuate cell death by inhibiting apoptotic signal-regulated kinase 1 and P53-related apoptotic pathways (23,24).

Autophagy is a catabolic process involving the formation and targeted degradation of autophagosomes in cells, which aims to support the recycling and energy regeneration of intracellular nutrients. In addition to non-selective degradation, mitophagy is a type of selective autophagy that removes damaged mitochondria and maintains a healthy mitochondrial network (25). It is used to maintain homeostasis in the intracellular environment and is significantly related to the level of oxidative stress *in vivo* (4). PTEN is one of the main downstream molecules involved in the regulation of the DJ-1 protein (26). PINK1 is a serine/threonine kinase that recruits Parkin through phosphorylation; Parkin is an intracellular E3 ubiquitin-protein ligase that targets ubiquitinated outer mitochondrial membrane and induces mitochondrial autophagy (27). Oxidized DJ-1 can closely bind to PTEN and inhibit its function, thereby increasing the phosphorylation activity of PI3K/Akt (28), which is another mechanism by which DJ-1/PTEN participates in autophagy regulation.

DJ-1 was first discovered in a study of the pathogenesis of Parkinson's disease (29); therefore, it is also called Parkinson's protein. Previous studies on DJ-1 function have mainly focused on neurodegenerative diseases, such as Parkinson's disease (30,31). However, its pathophysiological role in the kidneys remains largely unknown. Few studies have focused on systemic diseases involving glomeruli and renal tubules, mainly in *in vitro* cell and animal experiments, such as diabetic nephropathy (32), hypertensive nephropathy (33), infectious renal failure (34,35) and ischemia/reperfusion renal injury (36). Therefore, the present study aimed to explore the role of DJ-1 in the pathogenesis of primary kidney disease.

The results of the present study demonstrated that the morphology and structure of podocytes in the Si-DJ-1 group were worse than those in the control group, and the number was markedly reduced, whereas the morphology and number of podocytes in the OE-DJ-1 group were not noticeably different from those in the control group. The apoptotic rate of podocytes in the Si-DJ-1 group was markedly increased compared with that in the control group, whereas that in the OE-DJ-1 group was lower. It could be hypothesized that DJ-1 may be an effective protective protein in glomerular podocytes, and could serve an important role in maintaining their normal morphology and structure. Silencing the DJ-1 gene may affect the normal proliferation and metabolism of podocytes, leading to an increase in their apoptotic rate. Under a transmission electron microscope, the morphology and structure of mitochondria in the OE-DJ-1 group were shown to be intact, and there was no marked difference compared with the control group. In the Si-DJ-1 group, the mitochondrial structure swelled, cristae dispersed, vacuoles appeared and the number of autophagosomes was increased. It is suggested that increasing the expression of DJ-1 may reduce the level of mitochondrial autophagy in podocytes to some extent. PTEN is an important protein phosphatase in the human body that regulates mitochondrial autophagy by increasing protein phosphorylation in signal transduction pathways, such as PI3K/Akt and PINK/Parkin. The present study confirmed that DJ-1 can negatively regulate the expression of PTEN. Combined with all of the present experimental results, it was deduced that PTEN may be one of the main downstream molecules in the DJ-1-regulated signal transduction pathway. DJ-1 may regulate mitochondrial autophagy and participate in podocyte protection via PTEN, which is consistent with previous reports. Overexpression of the DJ-1 gene and reduction of PTEN expression can reduce the mitochondrial autophagy in podocytes, maintain healthy and complete morphological structure of mitochondria, stabilize the effective energy supply of mitochondria, and protect the normal function of podocytes. By contrast, silencing the DJ-1 gene can increase the expression of PTEN, leading to excessive mitochondrial autophagy, which cannot ensure normal energy supply, thus leading to podocyte damage.

It is well known that podocyte injury leads to glomerular filtration membrane dysfunction, one of the main causes of proteinuria. Few studies have examined the relationship between mitochondrial autophagy and glomerular podocyte injury. Our research group has explained this relationship in detail in previous studies. Yu and Yu (37) suggested that autophagy is involved in the damage of glomerular podocytes caused by puromycin, which is closely related to the damage and repair of podocytes. Xie and Yu (38) reported that the mitochondrial autophagy process mediated by the PINK1/Parkin signaling pathway is affected by a number of other proteins and related signaling pathways at the same time, so as to protect podocytes from external damage. Yang *et al* (39) revealed that by increasing the expression of autophagy-related protein LC3 and enhancing the autophagy activity of glomerular podocytes, they can significantly reduce the damage to glomerular podocytes in mice induced by puromycin, reduce the production of proteinuria and delay glomerular sclerosis. These findings suggest that increasing autophagy may be an effective protective mechanism of podocytes under the condition of injury. DJ-1 is a sensitive oxidative stress receptor. It participates in the development of various diseases by regulating mitochondrial autophagy. As an essential organ with active energy metabolism in the body, oxidative damage to the kidneys is a common factor in the occurrence of glomerular diseases. Podocytes are rich in mitochondria. Autophagy is an important process that affects growth, metabolism, apoptosis and function. Therefore, we hypothesized that the DJ-1 protein could protect podocytes and reduce the occurrence of proteinuria by regulating mitophagy. Combined with previous research on the DJ-1/PTEN pathway and the results of the present study, it may be suggested that DJ-1 participates in regulating mitochondrial autophagy through the DJ-1/PTEN pathway. On the one hand, DJ-1 may directly combine with excessive ROS in podocytes through its own unique structure to serve an antioxidative stress function; on the other hand,

mitochondrial damage may be reduced by reducing excessive autophagy and ineffective autophagy of podocyte mitochondria. As a result, the normal energy supply of podocytes can be ensured, morphological and functional damage of glomerular podocytes can be avoided, and the formation of urinary protein can be reduced.

Subsequently, we aim to establish a podocyte injury model and conduct quantitative analysis of DJ-1 in the experimental group to assess the protective function of DJ-1 on podocytes under the condition of kidney disease. There are other limitations in the present study. Without a three-dimensional internal experiment, it is not possible to accurately evaluate the function of DJ-1 *in vivo*, and this will be improved on in subsequent experiments.

In conclusion, under the condition of overexpression or silencing of the DJ-1 gene, the present study assessed its effects on mitochondrial autophagy, podocyte morphology and apoptosis. When the DJ-1 gene was silenced, the level of mitophagy in glomerular podocytes was increased significantly, the expression of the autophagy marker protein LC3B was increased, and podocytes exhibited excessive mitophagy and an increased apoptosis rate. These findings indirectly indicated that DJ-1 may protect podocyte function by regulating mitophagy. Therefore, DJ-1 may be considered a new target for the treatment of kidney diseases caused by mitochondrial autophagy-mediated podocyte injury.

Acknowledgements

Not applicable.

Funding

The present study was funded by the Science Foundation of Guangzhou First People's Hospital (grant no. M2019020), the National Natural Science Foundation of China (grant nos. 81273205 and 81670652), the Guangdong Planned Project of Science and Technology (grant no 2016A020215010), the Youth Cultivation Fund of Guangdong Medical University (grant no. GDMUQ2022008) and the Project of Guangdong Medical Science and Technology Research Fund (grant no. A02022128).

Availability of data and materials

The datasets used and/or analyzed during the current study are available from the corresponding author on reasonable request.

Authors' contributions

JX was involved in data analysis and writing. GL and LY performed conceptualization, validation, supervision, and reviewed and edited the manuscript. JT and SY were involved in collecting experimental data and software application. JX and JT confirm the authenticity of all the raw data. All authors read and approved the final manuscript.

Ethics approval and consent to participate

Not applicable.

Patient consent for publication

Not applicable.

Competing interests

The authors declare that they have no competing interests.

References

1. Mukherjee K, Gu C, Collins A, Mettlen M, Samelko B, Altintas MM, Sudhini YR, Wang X, Bouley R, Brown D, *et al*: Simultaneous stabilization of actin cytoskeleton in multiple nephron-specific cells protects the kidney from diverse injury. Nat Commun 13: 2422, 2022.
2. Gourlay CW, Carpp LN, Timpson P, Winder SJ and Ayscough KR: A role for the actin cytoskeleton in cell death and aging in yeast. J Cell Biol 164: 803-809, 2004.
3. Oh SE and Mouradian MM: Regulation of signal transduction by DJ-1. Adv Exp Med Biol 1037: 97-131, 2017.
4. Palikaras K, Lionaki E and Tavernarakis N: Mechanisms of mitophagy in cellular homeostasis, physiology, and pathology. Nat Cell Biol 20: 1013-1022, 2018.
5. Li G, Yang J, Yang C, Zhu M, Jin Y, McNutt MA and Yin Y: PTEN α regulates mitophagy and maintains mitochondrial quality control. Autophagy 14: 1742-1760, 2018.
6. Qiu L, Ma Z, Li X, Deng Y, Duan G, Zhao LE, Xu X, Xiao L, Liu H, Zhu Z and Chen H: DJ-1 is involved in the multidrug resistance of SGC7901 gastric cancer cells through PTEN/PI3K/Akt/Nrf2 pathway. Acta Biochim Biophys Sin (Shanghai) 52: 1202-1214, 2020.
7. Li H, Hu X, Ma B and Zhang H: Effect of Parkinson's disease-relevant protein DJ-1 on cell proliferation, apoptosis, invasion and migration in human osteosarcoma cells. Zhong Nan Da Xue Xue Bao Yi Xue Bao 43: 1054-1060, 2018 (In Chinese).
8. Ma Z, Yang J, Yang Y, Wang X, Chen G, Shi A, Lu Y, Jia S, Kang X and Lu L: Rosmarinic acid exerts an anticancer effect on osteosarcoma cells by inhibiting DJ-1 via regulation of the PTEN-PI3K-Akt signaling pathway. Phytomedicine 68: 153186, 2020.
9. Wang L, Lu G and Shen HM: The long and the short of PTEN in the regulation of mitophagy. Front Cell Dev Biol 8: 299, 2020.
10. Tan JJ, Yu SY, Zhang Y, Hao ZH and Yu L: Effect of tacrolimus on the expression of Park7 in glomerular podocytes injured by puromycin aminonucleoside. Zhongguo Dang Dai Er Ke Za Zhi 23: 951-958, 2021 (In Chinese, English).
11. Yin L, Li H, Liu Z, Wu W, Cai J, Tang C and Dong Z: PARK7 protects against chronic kidney injury and renal fibrosis by inducing SOD2 to reduce oxidative stress. Front Immunol 12: 690697, 2021.
12. Wu F, Li S, Zhang N, Huang W, Li X, Wang M, Bai D and Han B: Hispidulin alleviates high-glucose-induced podocyte injury by regulating protective autophagy. Biomed Pharmacother 104: 307-314, 2018.
13. Bo YY, Liang LD, Hua YJ, Zhao Z, Yao MS, Shan LB and Liang CZ: High-purity DNA extraction from animal tissue using picking in the TRIzol-based method. Biotechniques 70: 186-190, 2021.
14. Livak KJ and Schmittgen TD: Analysis of relative gene expression data using real-time quantitative PCR and the 2(-Delta Delta C(T)) method. Methods 25: 402-408, 2001.
15. Zhao M, Altankov G, Grabiec U, Bennett M, Salmeron-Sanchez M, Dehghani F and Groth T: Molecular composition of GAG-collagen I multilayers affects remodeling of terminal layers and osteogenic differentiation of adipose-derived stem cells. Acta Biomater 41: 86-99, 2016.
16. Wang X, Gan H and Du X: High glucose induces podocyte apoptosis and constitutive photomorphogenic 1 expression changes. CRTER 15: 4461-4464, 2011.
17. Ge M, Molina J, Kim JJ, Mallela SK, Ahmad A, Varona Santos J, Al-Ali H, Mitrofanova A, Sharma K, Fontanesi F, *et al*: Empagliflozin reduces podocyte lipotoxicity in experimental Alport syndrome. Elife 12: e83353, 2023.
18. Cheng Y, Marion TN, Cao X, Wang W and Cao Y: Park 7: A novel therapeutic target for macrophages in sepsis-induced immunosuppression. Front Immunol 9: 2632, 2018.

19. Bahmed K, Boukhenouna S, Karim L, Andrews T, Lin J, Powers R, Wilson MA, Lin CR, Messier E, Reisdorph N, *et al*: The effect of cysteine oxidation on DJ-1 cytoprotective function in human alveolar type II cells. Cell Death Dis 10: 638, 2019.
20. Song IK, Kim MS, Ferrell JE Jr, Shin DH and Lee KJ: Stepwise oxidations play key roles in the structural and functional regulations of DJ-1. Biochem J 478: 3505-3525, 2021.
21. Zhang L, Wang J, Wang J, Yang B, He Q and Weng Q: Role of DJ-1 in immune and inflammatory diseases. Front Immunol 11: 994, 2020.
22. Neves M, Grãos M, Anjo SI and Manadas B: Modulation of signaling pathways by DJ-1: An updated overview. Redox Biol 51: 102283, 2022.
23. Zhang XL, Wang ZZ, Shao QH, Zhang Z, Li L, Guo ZY, Sun HM, Zhang Y and Chen NH: RNAi-mediated knockdown of DJ-1 leads to mitochondrial dysfunction via Akt/GSK-3ß and JNK signaling pathways in dopaminergic neuron-like cells. Brain Res Bull 146: 228-236, 2019.
24. Niki T, Endo J, Takahashi-Niki K, Yasuda T, Okamoto A, Saito Y, Ariga H and Iguchi-Ariga SMM: DJ-1-binding compound B enhances Nrf2 activity through the PI3-kinase-Akt pathway by DJ-1-dependent inactivation of PTEN. Brain Res 1729: 146641, 2020.
25. Ali T, Hussain F, Kayani HUR, Naeem M and Anjum F: The role of mitochondria and mitophagy in cell senescence. Adv Protein Chem Struct Biol 136: 93-115, 2023.
26. Oswald MC, Brooks PS, Zwart MF, Mukherjee A, West RJ, Giachello CN, Morarach K, Baines RA, Sweeney ST and Landgraf M: Reactive oxygen species regulate activity-dependent neuronal plasticity in Drosophila. Elife 7: e39393, 2018.
27. Li W, Du M, Wang Q, Ma X, Wu L, Guo F, Ji H, Huang F and Qin G: FoxO1 promotes mitophagy in the podocytes of diabetic male mice via the PINK1/Parkin pathway. Endocrinology 158: 2155-2167, 2017.
28. Yu S and Yu L: The mechanism of PI3K/Akt signaling pathway in the apoptosis of glomerular podocytes. J Pediatr Pharm 25: 1-5, 2019 (In Chinese).
29. Dolgacheva LP, Berezhnov AV, Fedotova EI, Zinchenko VP and Abramov AY: Role of DJ-1 in the mechanism of pathogenesis of Parkinson's disease. J Bioenerg Biomembr 51: 175-188, 2019.
30. Heremans IP, Caligiore F, Gerin I, Bury M, Lutz M, Graff J, Stroobant V, Vertommen D, Teleman AA, Van Schaftingen E and Bommer GT: Parkinson's disease protein PARK7 prevents metabolite and protein damage caused by a glycolytic metabolite. Proc Natl Acad Sci USA 119: e2111338119, 2022.
31. Imberechts D, Kinnart I, Wauters F, Terbeek J, Manders L, Wierda K, Eggermont K, Madeiro RF, Sue C, Verfaillie C and Vandenberghe W: DJ-1 is an essential downstream mediator in PINK1/parkin-dependent mitophagy. Brain 145: 4368-4384, 2022.
32. Das F, Dey N, Venkatesan B, Kasinath BS, Ghosh-Choudhury N and Choudhury GG: High glucose upregulation of early-onset Parkinson's disease protein DJ-1 integrates the PRAS40/TORC1 axis to mesangial cell hypertrophy. Cell Signal 23: 1311-1319, 2011.
33. Cuevas S, Yang Y, Konkalmatt P, Asico LD, Feranil J, Jones J, Villar VA, Armando I and Jose PA: Role of nuclear factor erythroid 2-related factor 2 in the oxidative stress-dependent hypertension associated with the depletion of DJ-1. Hypertension 65: 1251-1257, 2015.
34. Leeds J, Scindia Y, Loi V, Wlazlo E, Ghias E, Cechova S, Portilla D, Ledesma J and Swaminathan S: Protective role of DJ-1 in endotoxin-induced acute kidney injury. Am J Physiol Renal Physiol 319: F654-F663, 2020.
35. Yao Y, Wei H, Liu L, Liu L, Bai S, Li C, Luo Y, Zeng R, Han M, Ge S and Xu G: Upregulated DJ-1 promotes renal tubular EMT by suppressing cytoplasmic PTEN expression and Akt activation. J Huazhong Univ Sci Technolog Med Sci 31: 469, 2011.
36. Yin J, Xu R, Wei J and Zhang S: The protective effect of glutaredoxin 1/DJ-1/HSP70 signaling in renal tubular epithelial cells injury induced by ischemia. Life Sci 223: 88-94, 2019.
37. Yu-Shengyou and Li Y: Dexamethasone inhibits podocyte apoptosis by stabilizing the PI3K/Akt signal pathway. Biomed Res Int 2013: 326986, 2013.
38. Xie Q and Yu L: The role of Pink1/Parking signaling pathway in Pink1 gene silencing-mediated mitochondrial dysfunction in glomerular podocytes. Chin J Pract Pediatr 33: 347-352, 2018 (In Chinese).
39. Yang XQ, Yu SY, Yu L, Ge L, Zhang Y, Hao ZG and Liu GS: Effects of tacrolimus on autophagy protein LC3 in puromycin-damaged mouse podocytes. J Int Med Res 48: 300060520971422, 2020.